minerals

MDPI

Article

Archaeometry of a Roman Millstone from Santa Maria Arabona, Manoppello (Abruzzo, Central Italy)

Francesca Falcone [1,*], Anna Dionisio [2], Francesca Castorina [3], Angela Tufo [1], Rachel Elaine Francis [4] and Francesco Stoppa [1]

[1] Department of Psychological, Health and Territory Sciences, D'Annunzio University, 66100 Chieti, Italy; angelatufo@virgilio.it (A.T.); fstoppa@unich.it (F.S.)
[2] Soprintendenza Archeologia, Belle Arti e Paesaggio dell'Abruzzo, 66100 Chieti, Italy; anna.dionisio@beniculturali.it
[3] Dipartimento di Scienze della Terra, Università degli Studi di Roma "Sapienza", 00185 Roma, Italy; francesca.castorina@uniroma1.it
[4] Department of Arts Humanities and Social Sciences, Johnson County Community College, 12345 College Blvd, Overland Park, KS 66210, USA; Racheldicamillo@gmail.com
* Correspondence: francesca.falcone@unich.it

Abstract: A well-preserved Pompeiian-type millstone fragment was retrieved from the chance discovery of Roman ovens dating to the V-VI century BCE in the area of Santa Arabona Manoppello in Italy. This is the first evidence of an hourglass millstone in Abruzzo. This fragment was analyzed through petrography, geochemistry, statistical analyses, and radiogenic isotopes at the University G. d'Annunzio. The source location of the stones was narrowed down to the areas of Etna, Roccamonfina, and Vulsini due to the petrography, geochemistry, and statistical data elaboration of leucititic and basaltic rocks from Central Italy and Sicily. The accurate identification of the provenance of the stone used to produce the millstone results in a better understanding of commercial trade routes and Roman entrepreneurship throughout Italy. The correlation between the production site and its stones' dispersion throughout the Roman Empire is of great interest for understanding the vast network of Roman roads, their manageability of commerce, and the organization of their products to the outlying areas of their Empire and in the case of this discovery, specifically to the area of Abruzzo Italy.

Keywords: Roman hourglass mills; archaeometry; statistical analysis; rock-source; trade routes

Citation: Falcone, F.; Dionisio, A.; Castorina, F.; Tufo, A.; Francis, R.E.; Stoppa, F. Archaeometry of a Roman Millstone from Santa Maria Arabona, Manoppello (Abruzzo, Central Italy). *Minerals* **2021**, *11*, 948. https://doi.org/10.3390/min11090948

Academic Editor: Petrus J Le Roux

Received: 3 August 2021
Accepted: 27 August 2021
Published: 30 August 2021

1. Introduction

In 2013 and 2014, many terracotta fragments and lithic fragments emerged during some agricultural activities and a water pipe excavation, located at 14°3′20.84″ E longitude and 42°17′17.70″ N latitude in the Santa Maria Arabona area (Manoppello, Pescara province of Abruzzo, central Italy). The site is 500 m SW of an imperial age Roman villa [1].

The archaeological material is erratic, and was found at the ground surface, accumulated along a road and a few more in the nearby vineyard. Judging from the large dimensions of some wall fragments, they must have come from a short distance. After selecting sample fragments, the material was stored at Archaeometry and Microanalyses Center of the University G. d'Annunzio under permission of the Archaeological Authority of Abruzzo–Chieti (code MBAC-SBA-ABR prot. 000300917/04/2014). Most of the fragments are from large dolia, part of the structure of an oven, plus bipedalis (two-foot tile), bessales, tegulae, and imbrices. Another type is a segment of circular bricks belonging to a brick column or suspensurae. The dolia fragments found are rims, bases, walls, and lids. In addition, there are various fragments of fired ceramics and fragments of amphorae used as storage containers for wine, oil and grains. Among the stone elements, it is possible to identify cubilia made of sandstone used to implement the opus reticulatum and varieties

of marble laths. There are many different types of terracotta: some are rough with large chamotte fragments in the ceramic mixture. There are at least three types of groundmasses: purified, fine-grained terracotta groundmass, and coarse-grained inequigranular groundmass. Other groundmasses found are refined and of fine-grained material. The color difference is equally vast, indicating different temperatures of terracotta-firing. Some result in a black core due to insufficient oxidation of organic matter in the clay mixture. Carbonate presences indicate temperatures lower than 900 °C and scarce clay depuration. The most significant fragments come from sections of a furnace composed of imbrices bound together by a mortar made up of lime, clay, and cocciopesto. At the time of discovery, the fragments were mixed and reworked, thus making it impossible to reconstruct the fragments into a single object. Therefore, it is complex and highly speculative to hypothesize their original use, stratigraphy, and primary location. However, it can be assumed that they belonged to a late productive factory manufactured with reused material from the Roman villa.

Notably, among lithic fragments is a portion of an hourglass millstone, such as those prevalent in Pompeii. Only part of the central body, including a register in relief, was preserved, as was a square niche that welcomed wooden poles, placed in the catillus, for grinding cereals. The introduction of rotary motion in the milling process occurs in the western Mediterranean between the IV and III centuries BCE. There are two main types: the manual round mill and the hourglass grinder, also called the Pompeian type for the significant presence of millstones of this type in the ancient city of Pompeii [2]. The hourglass grinder is comprised of a lower conical stone called a meta and an upper one shaped like an open hourglass, or catillus (Figure 1f). The meta is fixed to a base at the central point of the height of the catillus, that of maximum narrowing. Two holes were drilled to fix the wooden poles to be used for the yoke of the draft animals (Figure 1a,c) [3]. At the center of the upper cone of the catillus, the hopper opened, in which grain was inserted to be reduced into flour. In general, this type of grinder was heavy, and often stationary [3]. It was designed to produce copious quantities of flour, and therefore, in the imperial age, it was used to meet the growing needs of large urban populations. This need also explains the use of compact, hard, and resistant igneous rocks. The alveolar surface made it easy for the ground floor to empty without assistance and without clogging the gear.

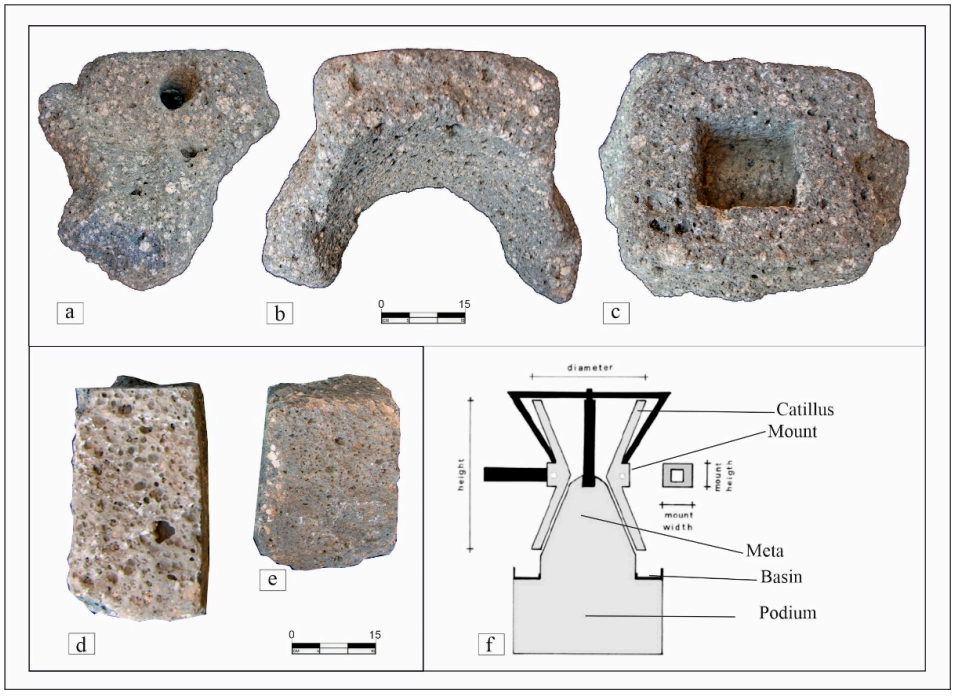

Figure 1. (**a**) L15 Manoppello millstone, lateral catillus; (**b**) L15, frontal catillus; (**c**) L15 lateral mount; (**d**) L14A podium; (**e**) L14B meta; (**f**) hourglass millstone structure.

1.1. Macroscopic Description and Archaeological Consideration

The Romans exploited various lava rock sources present in Italy. The most employed rocks are trachyte of the Euganean Hills volcanic district (Padua Veneto); leucite phonolite from the volcanic complex of Vulsini (Orvieto, Northern Lazio-Western Umbria regions); leucite-bearing trachy basalt from the Somma–Vesuvius volcano (Naples, Campania); tephrite foidites from the Mount Vulture volcano (Potenza, Basilicata); volcanic rocks from Sardinia, mainly rhyolitic ignimbrite from Mulargia, and mugearitic basalts from Etna (Catania, Sicily, Italy).

We investigated three artifacts that refer to millstones: L15 catillus, L14A segment of an hourglass millstone podium, and L14B meta fragments (Figure 1a–e) in relation to the hourglass millstone model structure in the literature [3].

A pioneering study of the Pompeii millstones was done by Peacock [4], who recognized leucite tephrite from Vesuvius and leucitite from the Vulsini volcanic area [5]. The principal rock types of Leucite-bearing rocks cover a vast composition from genuine leucitites (leucite > 60% in the AQPF diagram) to phono-tephrites and tephri-phonolites, to phonolites. It is not easy to assign a sure origin to these rock types, which are standard in the Roman region [6] and elsewhere in Italy. Source identification cannot be based on the petrographic description but need a complete petrological study.

Although the origin of the materials used in Roman times to produce millstones is generally known, identifying the quarries remains problematic. In fact, due to nearly 2000 years of continuous volcanic activity from Vesuvius and Etna, many of these quarries were completely obliterated [7]. Another problem is that the volcanic formations do not have lateral continuity and are often relatively small, so that the quarrying sites may have been abandoned after a relatively short period of use. Although numerous techniques allow us to identify lithotypes with precision, their origin often remains uncertain. In addition to more common petrological analysis, it is also possible to use the absolute chronology through K/Ar and Ar/Ar, but this type of investigation is costly, time-consuming, and consequently not frequently used. Radiogenic isotopic analyses (Sr/Nd) are also expensive and only give a general indication of the volcanic district to which the rock belongs. Bearing this in mind, our investigation was carried out on the samples found at Manoppello, based on exhaustive petrography, geochemistry, and isotopic geochemistry, implemented by statistical processing of the date. The petrological investigation took place on the millstone fragments based on a thin-section microscope optical SEM-EDS study, XRD mineral phase identification, and quantification. A set of major and trace elements was analyzed by multimethod analyses and statistically compared with a large dataset of alkaline rocks from Italy. The rock-type dataset was processed by principal-component and cluster analyses and plotted in conventional rock-type classification diagrams. Sr-Nd isotopic data further restricts the provenance of investigating rock-type geographical origin.

1.2. Methodology

Hourglass millstone rocks were studied by Zeiss and Phenom XL SEM optical microscopy, at the University G. d'Annunzio in Chieti, Chieti, Italy). BSE images were obtained using a Phenom XL SEM hosted at the Center for Advanced Studies and Technology at the University G. d'Annunzio of Chieti-Pescara. Powder XRD was carried out using the X-ray diffractometer Rigaku Miniflex II located at the DiSPUTer (Chieti, Italy). The acquisition parameters that were used in the XRD DiSPUTer-Uda laboratory at the University G. d'Annunzio, Chieti, Italy were Cu-K (1.540598 Å) radiation generated at 30 kV and 15 mA in an exploratory interval between 3 and 70 2ϑ, 0.1 steps, and a scan rate of 0.15/s. Once the diffractogram was obtained, background subtraction, and indexing of peaks with semi-quantitative analysis were performed. Mineral identification was performed using Match 3 software. Whole-rock geochemistry was performed at ActaLabs (Activation Laboratories, Ancaster, ON, Canada) by lithium metaborate/tetraborate fusion FUS-ICP for whole rocks and FUS-MS for trace elements. FeO was detected by titration. Isotopic analyses were carried out using Finnigan MAT 262RPQ multicollector and Micromass

VG 54E single collector mass spectrometers. Internal precision (within-run precision) of a single analytical result is given as two standard errors of the mean (2 se). Repeated analyses of standards gave averages and errors expressed as 2 standard deviation (2s) as follows: NBS 987, 87Sr/86Sr = 0.710237 + 10 (n = 20), 86Sr/88Sr normalized to 0.1194; La Jolla, 143Nd/144Nd = 0.512875 + 10 (n = 15), 146Nd/144Nd normalized to 0.7219.

1.3. Petrography and Petrology

The L14A rock sample shows a seriate porphyritic texture with anhedral and subhedral olivine phenocrysts in an intersertal (glassy mesostasys) or intergranular (ophitic) textured groundmass. Zoned plagioclase phenocrysts form abundant large euhedral laths sometimes arranged in glomeroporphyric structures, Microlaths of plagioclase frame, euhedral clinopyroxenes, olivine grains, nepheline, and K-feldspar. Pheno-mode suggests olivine alkali basalt. SEM-EDS analyses confirm andesine in phenocrysts, oligoclase in microphenocrystals, and much lesser K-feldspar and nepheline. Mafic minerals were dominated by olivine (Fo_{54}), containing a small amount of Mn and Ca less (than 1%), and augite (Wo 36%, En 51%, Fs 12%). Opaques were mainly ulvösplinel (TiO_2 up to 22 wt%) and magnetite. Accessory minerals were apatite and Ca-Mg carbonate (Figure 2a,b).

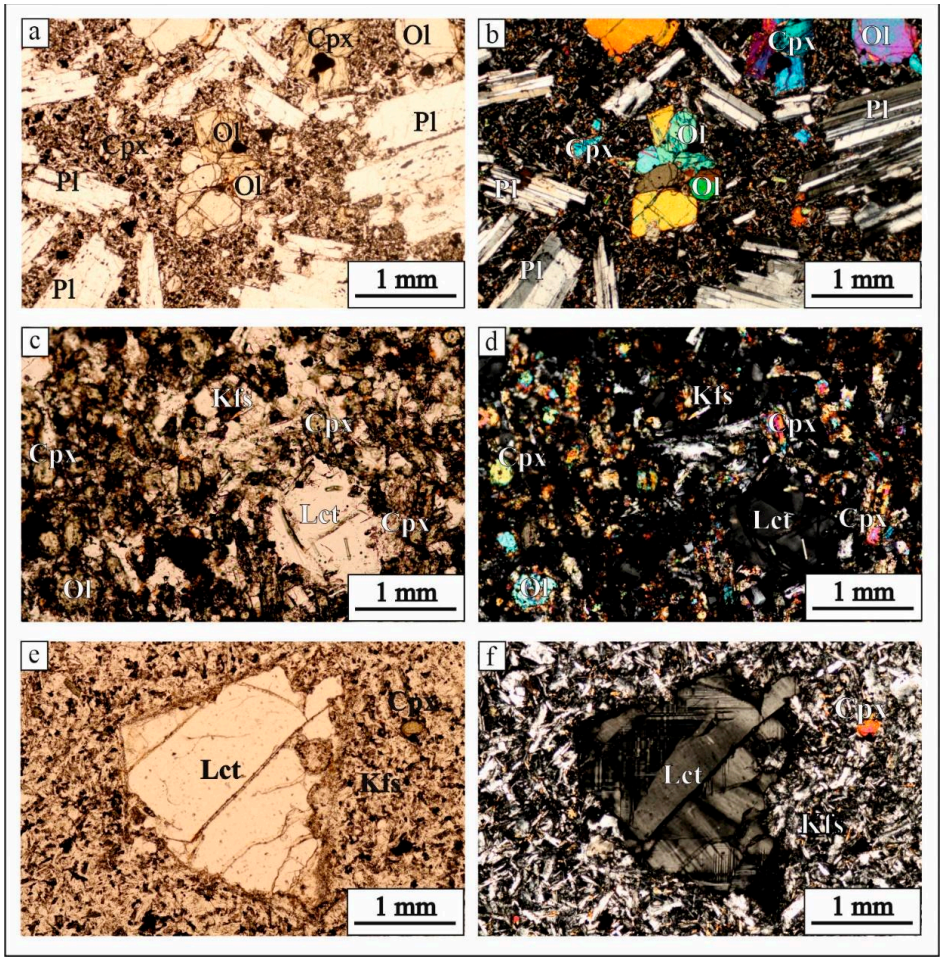

Figure 2. PL and XL picture of thin sections. (**a**,**b**) sample L14A: olivine alkali basalt, trachytoid texture with phenocrysts of plagioclase, olivine and pyroxene in a groundmass of K-feldspar, cpx and nepheline; (**c**,**d**) sample L14B: Leucititic phono tephrite: leucite phenocrysts in an interstitial intergranular groundmass of cpx, plagioclase, K-feldspar and nepheline; (**e**,**f**) Sample L15: leucitophyre showing large leucite phenocrysts immersed in a trachytic groundmass of K-feldspars, cpx.

The L14B sample was a seriate porphyritic rock with phenocrysts of euhedral zoned cpx (augite-diopside), leucite and olivine (chrysotile-hyalosiderite) in a groundmass of

abundant skeletal cpx laths, scarce plagioclase (oligoclase-andesine), and intergranular K-feldspar (sanidine, anorthoclase), nepheline (K_2O up to 1.72 vol%), and leucite. Accessory minerals were small andradite garnet, Ti-magnetite (TiO_2 13.2 vol%), and apatite (Figure 2c,d).

L15 is a porphyritic rock with large polysynthetic geminated leucite crystals and pyroxenes, zoned plagioclase rich in inclusions in a groundmass consisting of fluidly arranged laths of K-feldspar with intergranular cpx, leucite and opaques. The cpx were augites with TiO2 up to 2.35 vol%, olivine (Fo_{54}) containing MnO up to 0.8 vol%, and CaO 0.54 w%. Feldspar were sanidine plus anorthoclase, plagioclase was oligoclase to andesine (Figure 2e,f).

Sample L14A was a rock type not common in peninsular Italy, limited to Sicily and the Etna volcano. On the other hand, leucite-bearing rocks are typical of the Roman region and present in the Campania volcanic district and Roccamonfina and Vesuvius. Starting from this obvious consideration, it is possible to address the research on rocks from the locations mentioned above.

2. Major Element Geochemistry

Sample analyses are given in Table 1.

Table 1. Major elements, trace elements, rare earth elements of samples L14A, L14B, L15.

Major Elements				Trace Elements			
Wt.%	**L14A**	**L14B**	**L15**	**ppm**	**L14A**	**L14B**	**L15**
SiO_2	48.1	47.8	55.1	Y	23	27	39
TiO_2	1.65	0.83	0.47	Zr	223	255	667
Al_2O_3	16.8	16.5	19.4	Nb	49	15	49
Fe_2O_3	11.1	7.70	2.34	Cs	<0.5	32.1	19.2
MnO	0.17	0.14	0.13	Ba	835	1245	2444
MgO	5.15	4.91	0.80	Hf	4.3	5.4	11.3
CaO	9.97	11.2	3.94	Ta	2.8	0.8	2.5
Na_2O	3.75	1.91	2.95	Pb	3510	225	224
K_2O	1.68	6.08	9.34	Th	12.6	34.1	150
P_2O_5	0.56	0.33	0.14	**Rare Earth Elements**			
LOI	0.36	1.70	2.70	La	99.8	92.2	200
Total	99.4	99.2	99.4	Ce	173	182	354
Trace Elements				Pr	18.2	20.6	35.3
ppm	**L14A**	**L14B**	**L15**	Nd	65.9	75.3	113
Sc	21	21	2	Sm	11.4	14.4	17.4
V	282	199	123	Eu	3.03	3.01	3.47
Cr	70	70	-	Gd	8.30	10.4	10.0
Co	35	25	5	Tb	1.00	1.20	1.40
Ni	60	50	-	Dy	5.44	6.11	7.55
Cu	120	90	10	Ho	0.99	1.00	1.33
Zn	410	60	110	Er	2.66	2.70	3.80
Ga	21	17	21	Tm	0.35	0.36	0.57
Rb	32	448	320	Yb	2.22	2.220	3.77
Sr	910	1299	2031	Lu	0.31	0.31	0.61

Major elements of samples L14A, L14B, and L15 plotted in the conventional total alkali-silica (TAS) diagrams classified as trachy basalt, phono tephrite, and phonolite. In the de La Roche diagram (R1-R2) they classified as alkali-basalt, tephritic basanite and trachy-phonolite, respectively (Table 2). Classification using major elements may be inconsistent in the various diagrams for the petrographic observation. Due to the microcrystalline nature of the rocks, because it was impossible to calculate a modal composition, we used the virtual moda deduced by the CIPW norm calculation.

Table 2. Rock-type identification of samples L14A, L14B, L15.

	Rock-Type			
Sample	**TAS**	**R1-R2**	**AQPF (CIPW)**	**AQPF (XRD)**
L14A	trachy basalt	alkali-basalt	phonolitic tephrite	phonolitic tephrite
L14B	phono tephrite	tephritic basanite	phonolitic tephrite	phonolitic tephrite
L15	phonolite	trachy phonolite	tephritic phonolite	tephritic phonolite

L14A CIPW norm gave Ab 22.8%, An 24.6 vol%, Or 10.1 vol%, Ne 5.2 vol%, Di 18.3 vol%, Ol 12.5 vol%, Il 3.3 vol%, Mt 2.0 vol%, and Ap 1.3 vol%.

L14B CIPW norm gave An 20.0 vol%, Or 17.2 vol%, Ne 9.04 vol%, Lc 15.5, Di 29.5 vol%, Ol 5.69 vol%, Il 1.63 vol%, Mt 1.38 vol%, and Ap 0.78 vol%. The rocks classify as phono tephrite in the AQPF diagram.

L15 CIPW norm gave Ab 11.7 vol% A 19,0 vol%, Or 58.4 vol%, Ne 7.95 vol%, Di 5.6 vol%, Ol 1.5 vol%, Il 0.95 vol%, Mag 0.49 vol%, and Ap 0.34 vol%.

We implemented the norm calculation with an X-ray diffraction analysis (XRD), which only allows a semi-quantitative estimation of the multiphase mineral association. However, the estimation can be calibrated with a detailed petrographic description and the rock's virtual moda (CIPW norm).

L14A XRD gave sanidine 15.0 vol%, plagioclase 54.9 vol%, nepheline 14.5 vol%, augite 10.0 vol%, and olivine 5.6 vol%.

L14B XRD gave sanidine 34.8 vol%, plagioclase 21.9 vol%, nepheline 6.8 vol%, leucite 13.3 vol%, cpx 16.9 vol%, olivine 2.7 vol%, and Ti-magnetite 3.6 vol%.

L15 XRD gave plagiocalse 31.4 vol%, sanidine 20.1 vol%, nepheline 10.4 vol%, lucite 23.0 vol%, augite 11.6 vol%, and olivine 3.6 vol%.

A comparison between the sample CIPW norm and the XRD converge towards a more consistent classification of the rock type (Table 2). L14A and L14B classified as phonolitic tephrite, whereas L15 classified as tephritic phonolite in the AQPF diagram, both using CIPW norms and XRD (Table 2).

It is not easy, based only on petrographic description and major elements, to make a certain correspondence with already known rock-type sources. For example, Etna rocks are quite different from Roman region rocks, which contain abundant leucite. However, leucite-bearing rocks cover a vast composition from genuine leucitites (leucite > 60% in the AQPF diagram) to phono tephrites and tephri phonolites, to phonolites. Therefore, a statistical treatment can be more effective, but it needs a sufficiently large dataset built based on reasonable indication and the constraints offered by petrography and major element distribution.

2.1. Statistical Treatment

We approached the classification issue applying multiple statistical analyses on the 100 samples representative of the Italian rock composition, which were suitable candidates based on the preliminary petrographic investigation of samples L14A, L14B, and L15. The data set was built using a rock composition repository in the literature, plus a capillary research of rock analyses published elsewhere [8–23].

In our application, we used an advanced clustering method called HCPC (hierarchical clustering on principal components). This approach allowed us to combine the three standard methods used in multivariate data analyses [22]:

1. Principal component analyses (PCA).
2. Hierarchical clustering.
3. Partitioning clustering, particularly the k-means method.

All the analyses were performed on the statistical software R. We used the descriptive analyses to display the basic features of the data with the advantage of summarizing features of the samples, thus providing simple summaries about the samples and the measurements, which was very useful to present quantitative statistics in a manageable form, and to help to simplify large quantities of data in a sensible way. Differently from inferential methods, descriptive statistics describes what the data shows. A mixed approach using both methods was used in the paper [24]. However, we did not attempt any inferential statistical methods because they might have resulted in misleading conclusions that hide behind the immediate data. The boxplot is a purely graphical representation of chemical variability [25] (Figure 3a). In each boxplot, five parameters depict the chemical distribution of each element: minimum, first quartile (lower side of the box), median (black line in the box), third quartile (upper side of the box), and maximum. In the basic boxplot, the outliers are excluded (represented as empty circles in Figure 3a), and the minimum and maximum are the first and last data points, respectively, that are not considered outliers. Thus, the boxplot is helpful to establish whether the data is symmetric or asymmetric (skewed).

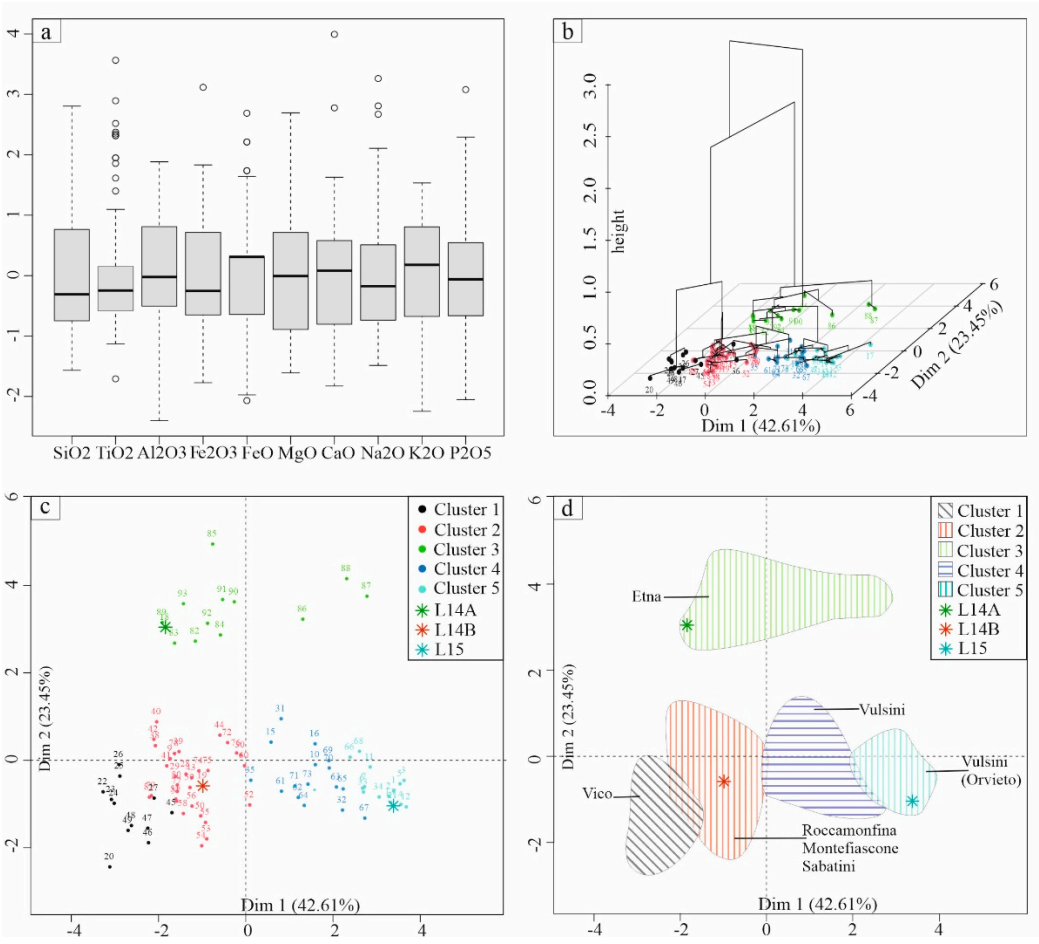

Figure 3. (**a**) Boxplot; (**b**) hierarchical clustering; (**c**) principal components analysis; (**d**) cluster analysis for a population of 100 rocks from literature selected as representative of potential sources of the investigated samples.

As in Reference [24], we plotted the results of the PCA in a biplot showing the first two principal components that explained most of the variability in the sample. Principal component analysis (PCA) is an exploratory data analysis for dimensionality reduction. It is the process of calculating the principal components and using them to perform a change of basis on the data. PCA is defined as an orthogonal linear transformation that projects the data to a new coordinate system such that the most significant variance by some scalar projection of the data comes to lie on the first coordinate (called the first principal component), the second greatest variance on the second coordinate, and so on, per Jolliffe (2005) [26]. For example, if we consider a matrix of quantitative data such as that defined by the chemical analysis of rocks, with a size of n samples $\times$ chemical variable ($n \times p$); and transform them into a new set of variables of the main components, the new set of k variables will have lower dimensionality than the original data set (typically k << p) and, being an orthonormal basis, each principal component is linearly uncorrelated with the others (mutually orthogonal). The first few principal components that explain most of the variance in the original data set were chosen for the graphical representation of igneous rocks analyses [27]. The component that explains the highest variance is reported on the x-axis, while the second highest is reported on the y axis (Figure 3c). Cluster analysis is one of the primary data mining techniques for exploring multivariate data sets. The goal is to divide the sample under examination into several clusters such that points in the same group share similar traits. There are multiple versions of cluster analysis. As far as distance measurements are concerned, in hierarchical clustering, the similarity between the clusters is calculated from dissimilarity measures like the Euclidean (or Mahalanobis) distance between clusters. There are many distance metrics that can be considered for the calculation of the dissimilarity measurement, and the choice depends on the type of data in the dataset. For the use of Mahalanobis distance as an outlier detection method, as in [24], we decided not to use it due to the assumptions needed on the distributive form of the data making that methodology inferential, and thus bearing the possibly of producing misleading results.

The algorithm of the HCPC method we used, as implemented in the FactoMineR package of R, follows these steps:

1. Compute principal components.
2. Compute hierarchical clustering: hierarchical clustering is performed using

Ward's criterion on the selected principal components. Ward's criterion is used in hierarchical clustering because it is based on multidimensional variances like the principal component analysis.

3. Choose the number of clusters based on the hierarchical tree; an initial partitioning is performed by cutting the hierarchical tree.
4. Perform K-means clustering to improve the initial partition obtained from hierarchical clustering. As a result, the final partitioning solution obtained after consolidation with k-means can be (slightly) different from the one obtained with the hierarchical clustering.

Hierarchical clustering was performed using Ward's criterion on the selected principal components [28]. Ward's criterion is used in hierarchical clustering because it is based on multidimensional variance (Dim1 42.61%; Dim2 23.45%) and reorders the measurements of the metric distance of the data (Figure 3b). Samples from the district of Vico were in cluster 1. Cluster 2 represents the districts of Roccamonfina, Montefiascone, and the Sabatini volcano complex. Cluster 3 is identified by samples from the volcanic district of Etna. In contrast, cluster 4 is comprised of the district of Vulsini, and cluster 5 presents only samples from the Orvieto district. The factor map indicates five main rock-type clusters. The study samples fit with L14B cluster 2 (Roccamonfina, Montefiascone, Sabatini volcanic complex), L14A cluster 3 (Etna), and L15 cluster 5 (Vulsini volcanic complex), respectively (Figure 3d).

To associate the statistical cluster with the rock-type of our data, we plotted the reference clusters into TAS [29], R1-R2 [30], CIPW normative, and AQPF diagrams [31] (Figure 4).

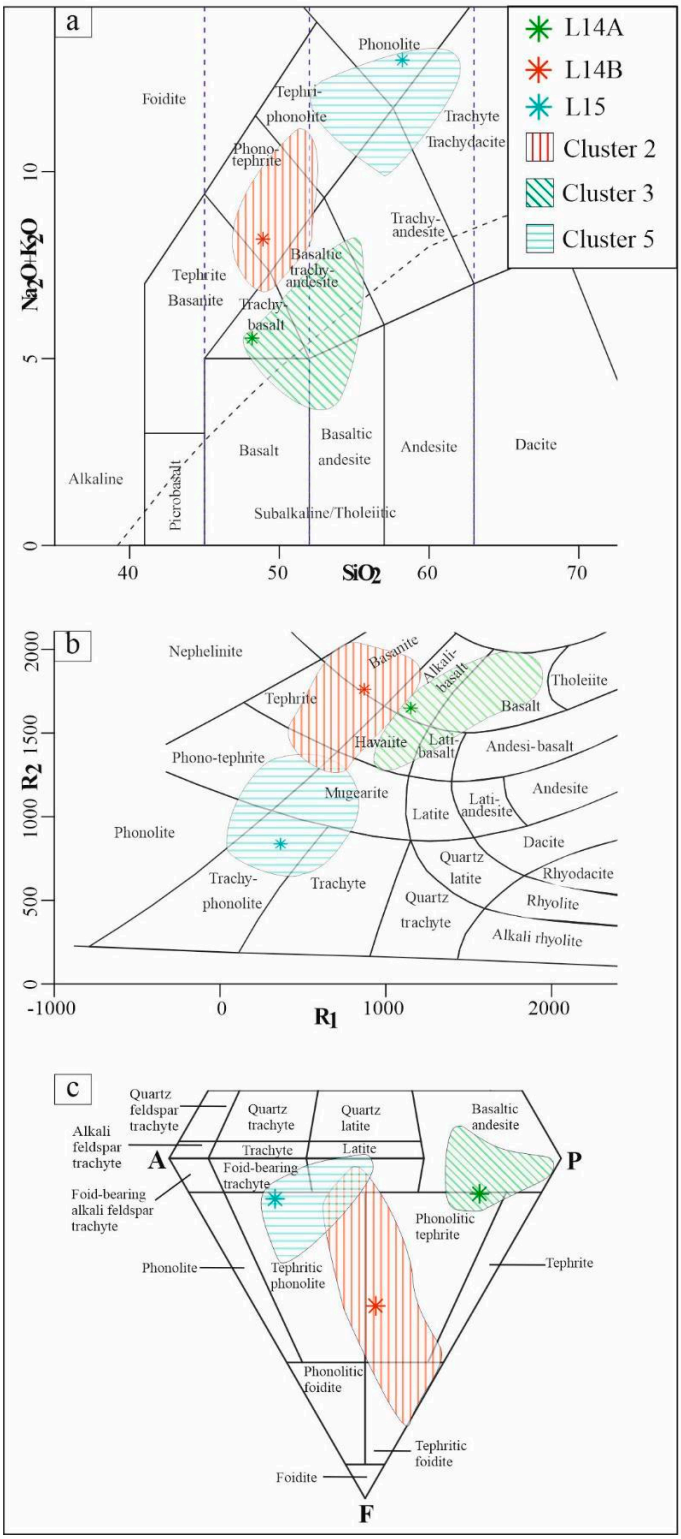

Figure 4. Conventional classification diagrams for major elements and modal composition of extrusive igneous rocks. (**a**) TAS; (**b**) R1-R2; (**c**) AQPF (modal classification of igneous rocks). The corners of the double triangle are A = alkali feldspar, P = plagioclase and F = feldspathoid.

2.2. Trace Element Geochemistry

Forty-five trace elements were determined in the investigated samples. Trace elements are plotted in conventional mantle-normalized spider diagrams in order of their compatibility (Figure 5a,c,e) [32]. REE are represented in chondrite-normalized multiphase diagrams (Figure 5b,d,f) [33].

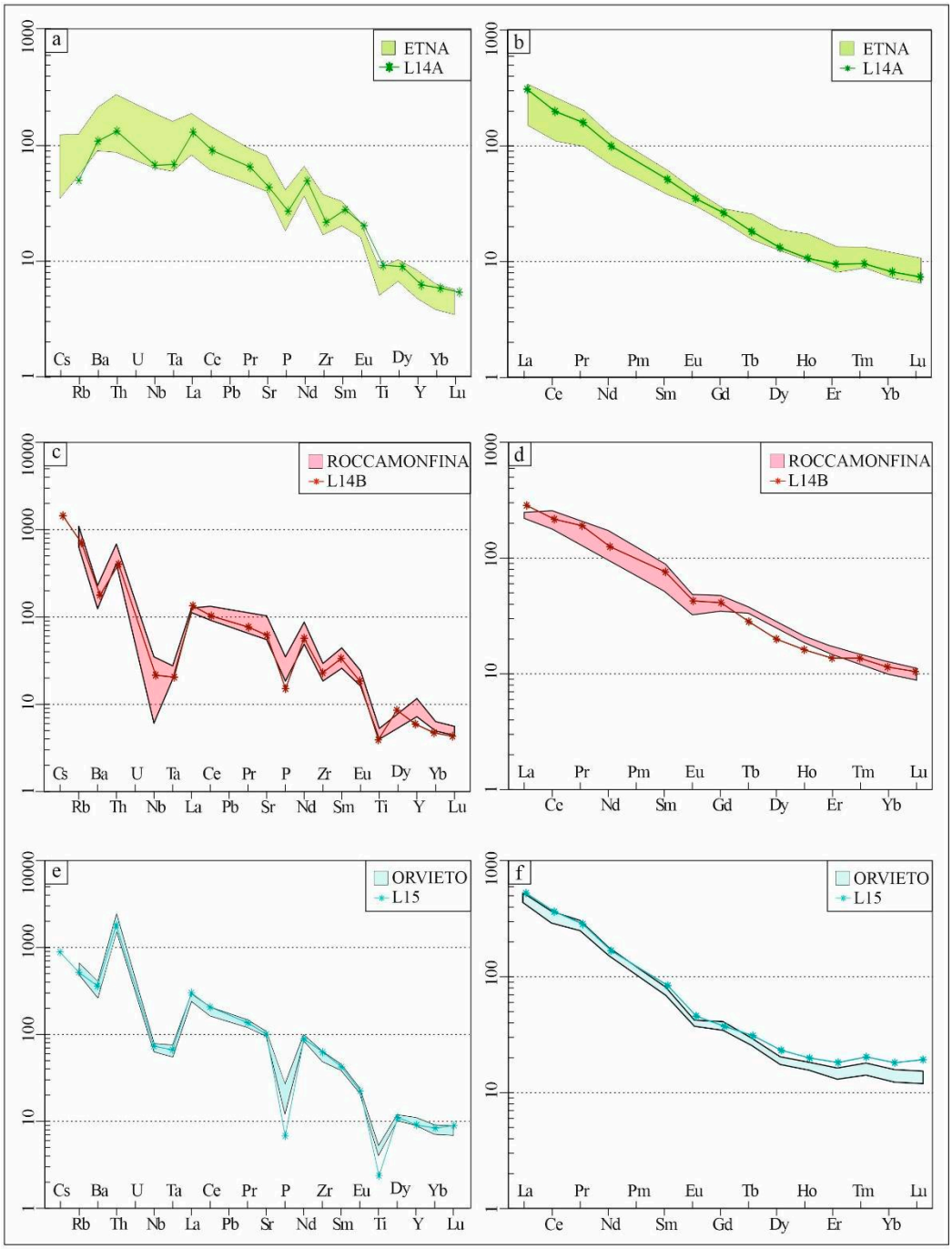

Figure 5. (**a**,**c**,**e**) Spider diagrams of elements normalized to primitive mantle and (**b**,**d**,**f**) REE chondrite, normalized, comparing investigated samples with statistically selected rock composition from the Etna, Roccamonfina, and Orvieto districts.

Sample L 14A has a flat or semi-bell-shaped trend of LILE and HFSE ranging from >100 mn for LILEs, LREE, and HFSE3+, between 100 and 10 for HFSE4+5+, and lower than 10 for HREE. A slight negative anomaly of P and Ti and a large Pb-positive anomaly is apparent. The plot of REE has a La/Luch equal to 26.6, with a slight Eu negative

anomaly (Figure 5a,b). L14B shows a high LILE/HFSE ratio with a decrease of compatible elements. It has negative anomalies of Nb-Ta, P, and Ti, and a moderate Pb-positive anomaly (Figure 5c,d). L15 shows a general enrichment of all the trace elements and a pattern similar to that of L14B. In addition, it is richer in REEs and has an apparent Th-positive anomaly (Figure 5e,f).

A marked difference in trace element geochemistry between sample L14A vs L14B and L15 is apparent. L14A fits well in the range of the Etna rocks. L14B and L15 have a negative Nb-Ta and Eu negative anomaly which is not apparent in the Etna rocks. L14B fits with the Roccamonfina leucite-bearing rocks, which have REE like the Etna rocks but an utterly different trace element distribution. L15 is characteristically enriched, like the other rocks of the Roman region, in REE, with a convex REE path. L15 fits particularly well with Vulsini complex rocks. (Figure 5) [8–23]. After comparing the trace elements, the provenance of the rocks is most likely Etna, Roccamonfina, and Vulsini (Orvieto), respectively.

2.3. Isotopic Geochemistry

Isotope geochemistry is a robust method to investigate the potential source of an igneous sample. The radiogenic isotope ratio does not change during magmatic evolution and reflects the source composition, which varies according to the different volcanic complexes. For example, Sr/Nd ratios are higher in the Roman region and gradually decrease towards the south [9,10,34,35]. Table 3 shows Sr and Nd isotopes data for each sample with the error standard (2se).

Table 3. Sr and Nd isotopes of samples L14A, L14B, and L15.

	Sr and Nd Isotope					
Sample	$^{87}Sr/^{86}Sr$	±	**2se**	$^{144}Nd/^{143}Nd$	±	**2se**
L14A	0.703702	±	0.000005	0.512986	±	0.000009
L14B	0.709366	±	0.000008	0.512261	±	0.000013
L15	0.711014	±	0.000007	0.512096	±	0.000009

The radiogenic isotopes Sr and Nd give a firm confirmation of the suggested provenance sites. Sample L14A fits with the Sr–Nd data from Etna. Sample L14B suggests Roccamonfina and sample L15 fits with the Vico and Vulsini leucitites (Figure 6). Thus, despite the isotopic analysis that excluded Vesuvius as a source for the rock, the L15 sample from the region of Rome could be attributed to coming from either Vico or Vulsini.

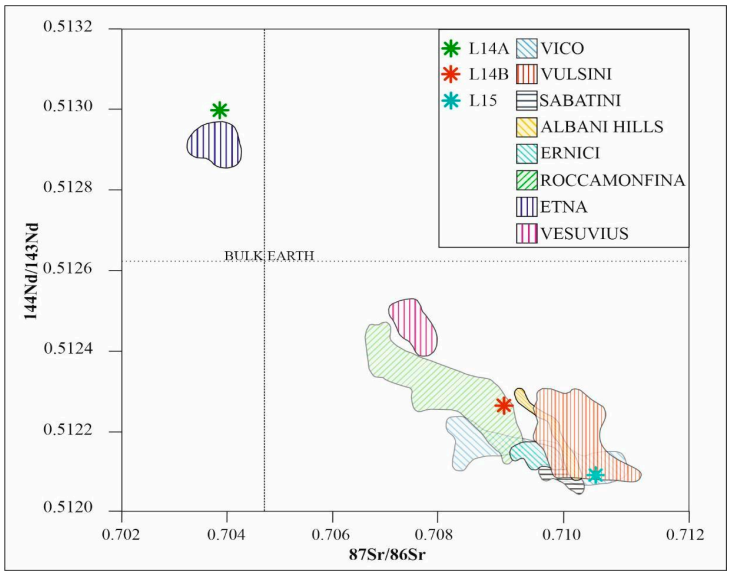

Figure 6. Radiogenic Isotopic Sr/Nd diagram [9,10,34,35].

2.4. Discussion

Romans exported hourglass millstone on a large scale. The widespread globalization of engineering and industrial techniques due to the road network and maritime transport made it possible to expand the market and offer a series of competitive products at a reasonable price that was worth transporting over long distances. The need to always have loads of ballast made it especially convenient to transport the millstones by sea, which explains why heavy objects could travel, for example, from Sicily to Rome and then be marketed within a reasonable radius of land transport. We cannot exclude that the sea routes were broader, allowing transport even along the coasts of the Adriatic. Furthermore, many rivers that are currently not navigable in Roman times were navigable, such as the Tiber River. Given the weight of these artifacts, it must be assumed that the rock was not only extracted, but also manufactured in or near the same extraction site, although there has hitherto been no evidence of this. So many ways are open to interpretation.

Concerning the Manoppello mills, we may hypothesize some different transportation routes. It is noteworthy that at about 10 km after the confluence with the Paglia river, there was an important crossroads of most of the trade of central Italy for the transport of leucite phonolite from the ancient quarry in the Orvieto area (Figure 7) [36,37]. This may account for the central collection point for the trade of Vulsini millstones along the Tiber [10,38], which was the natural watercourse for reaching the Tyrrhenian Sea [39–41]. However, the road that connects the city of Orvieto to Rome is the ancient Via Cassia, passing through Viterbo. In both cases, we guess that the millstone reached the Roman market and then was transported into central Italy to the east [5,42].

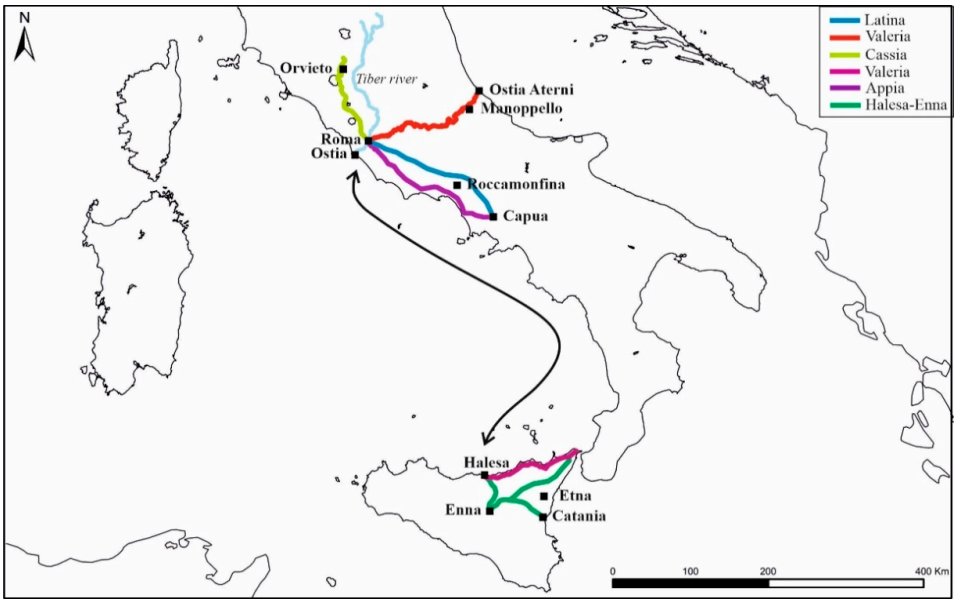

Figure 7. Roman trade routes for exporting lithic materials.

The lava rocks from the volcanic district of Roccamonfina may have travelled along the ancient Via Latina that connects Capua to Rome. From the port of Ostia Antica, built at the mouth of the Tiber River, some of the millstones coming from the volcanic district of the Vulsini could be quickly shipped (as cargo or as ballast) by different routes throughout the Mediterranean, including the distant provinces of the Roman Empire such as Gaul, Iberia, Tunisia, Tripolitania, and Cyrenaica [43]. Finally, the rocks coming from the Volcanic District of Etna may have been transported via the ancient Via Valeria, which connects Messina to Lilibeo and crosses with the innermost alternate route passing through Centuripe, which connects Messina, Catania, Enna and ends at the port of Halesa, known for its commerce [44–46]. Regardless of the location of the quarries and production centers, we suppose that the most reasonable hypothesis is that the millstones reached Rome and

from there were transported eastwards, reaching Manoppello and other localities along the Adriatic through the ancient Via Valeria (Claudia Valeria), which connects Rome to Ostia Aterni, passing through the city of Alba Fucens and Corfinium (Figure 7).

The lack of sure chronological markers makes the Santa Maria Arabona discovery difficult to precisely date. However, due to their heterogeneity, we deduce that the artifacts were derived from the spolia of the Roman Villa and re-used in a bakery. The materials analyzed do not come from a systematic stratigraphic excavation, but these are erratic finds waiting for a possible excavation. Excavation would allow identifying the mill's context in situ to hypothesize what may have been the causes of the re-use of its materials.

Earthquakes became a reference point in time that marked a period of abandonment and dispossession of the Roman Villa. The Majella area and the Chieti province suffered significant destruction during the Roman age with two earthquakes (II century AD and 484–508 AD) with epicenters in the region and another (346 CE) originating in the neighboring area [47]. Manoppello experienced significant damage in more recent earthquakes (1209, 1456, 1706, and 1933), suffering a maximum of XI degrees MCS of intensity in the earthquake of 1706. There is no doubt that the area is prone to elevated seismicity. Remarkable chronicled and archaeological data refer to the 100 AD earthquake (M ~6.2, IX M intensity, probably underestimated), which caused the collapse of buildings of the territorial district of Interpromium, near Manoppello. The account is recounted on a carved stone recycled to build the abbey of San Clemente da Casauria (871 CE). The inscription bears the commemoration of the restoration of Intrepromium's mensa ponderaria (public weighbridge) by two magistrates of Sulmona [48]. The I and IV–V century earthquakes correspond to major collapses or damage in all the archaeological sites of the Majella-Sulmona area. Although not thoroughly investigated, other possible evidence is the tilting of the thermal area of the Villa Rustica of Santa Maria Arabona and the collapse of other residential buildings in the surrounding area (unpublished excavation report by Manuela Rosati, archaeological superintendence of Chieti). However, we are sure that the Roman Villa was inhabited up to the III century CE. It seems the recovery of valuable tools such as the hourglass millstones occurred shortly after the IV–V century CE earthquake to reestablish grain production in an area essentially devoted to agriculture. The earthquake is the marker in time for previous Roman villa dispossession and their later conversion for agricultural use and grain mills. We consider the VI century CE to be the probable age of the bakery, utilizing the studied millstones.

3. Conclusions

The finding of artifacts related to hourglass mills found at Santa Maria Arabona revealed that hourglass mills derive from various locations and therefore are made from various stones. If the textural rock characteristics such as vesiculated surface with hard minerals and general rock homogeneity are similar, their geochemistry is different. Data consistency indicates that the lapicidae were able to identify and select similar lithotypes by empirical criteria based predominantly on the modal rock composition. It is not plausible to identify the source of the rocks using just petrography and conventional classification diagrams. More sophisticated statistical methods may help, as the inconsistencies need a double-check. Combining all the possible petrological features such as petrography, geochemistry, and isotopic geochemistry with statistical analyses, it was possible to hypothesize a probable origin of the rocks from three different localities—Etna, Roccamonfina, and very probably Vulsini. Samples L14A and B are consistent with Etna and Roccamonfina rocks, respectively. Sample L15 has some less obvious geographical locations. However, excluding the isotopic data, which do not allow a specific distinction between Vulsini and Vico, all the other data point to an origin from Vulsini and with leucitophyre from Sugano (Orvieto area). This paper offers an example of which methodologies may ensure a correct estimation of possible rock sources, overcoming petrographic uncertainty.

The most obvious result is that hourglass mills were widely commercialized, responding to market requests independently from the distance between the source and

the destination. Santa Maria Arabona, being on a main consular Roman street, th Tiburtine, suggests that the hourglass mills arrived from Rome, where they converged from the Roman region, Campania, and Etna. The market request minimized the high cost of transportation, indicating economic consumption influenced by the demand for better and more luxurious products. The archaeological context suggests the late re-use of the mills in a rural context with extensive evidence of the re-utilization of the republican villa. The presence of a bread oven, dolia, and ordinary fired ceramics is not undoubtedly related to the villa and may belong to an edifice whose basement is not exposed and requires excavation. The oven, dolia, and hourglass mills were unearthed while ploughing vineyard land and were located above the deck of a partially buried edifice. A major earthquake in the IV–V centuries CE may be a starting point in time for the re-utilization that occurred, dating the artifact to the V or VI century CE.

Author Contributions: Conceptualization, F.F., A.D., A.T. and F.S.; methodology, F.F. and F.S.; software, F.F. and F.S.; validation, F.F., F.S. and R.E.F.; formal analysis, R.E.F.; resources, F.S.; data curation, F.F., F.C. and F.S.; writing—original draft preparation, F.F., F.S., R.E.F. and A.D.; writing—review and editing, F.F., F.S. and R.E.F.; visualization, F.F., R.E.F. and F.S.; supervision, F.S.; project administration. F.S.; funding acquisition, F.S. All authors have read and agreed to the published version of the manuscript.

Funding: This research was funded by Francesco Stoppa, grant number 031307 Ateneo 2018/2019.

Data Availability Statement: Not applicable.

Acknowledgments: We thanks Fiorenzo Stoppa and Noemi Vicentini for statistical data suggestion and processing.

Conflicts of Interest: The authors declare no conflict of interest.

References

1. Staffa, R.A.; Odoardi, R.; Montanaro, M. Area archeologica in Contrada S. Maria Arabona di Manoppello. 2009. Available online: https://docplayer.it/55336182-Area-archeologica-in-contrada-s-maria-arabona-di-manoppello.html (accessed on 30 August 2021).
2. Amouretti, M.C. Decouvertes archeologiques recentes sur le moulins et pressoirs romains de Provence. In *Vivre, produire et échanger: Reflets méditerranéens (Mélanges offerts à Bernard Liou)*; Rivet, L., Sciallano, M., Eds.; Editions Monique Mergoil: Montagnac, France, 2002; pp. 465–469.
3. Buffone, L.; Lorenzoni, S.; Pallara, M.; Zanettin, E. The millstones of ancient Pompei: A petro-archaeometric study. *Eur. J. Miner.* **2003**, *15*, 207–215. [CrossRef]
4. Peacock, D.P. The production of Roman millstones near Orvieto, Umbria, Italy. *Antiqu. J.* **1986**, *66*, 45–51. [CrossRef]
5. Moritz, L.A. *Grain-Mills and Flour in Classical Antiquity*; Clarendon Press: Oxford, UK, 1958; p. 230.
6. Washington, H.S. *The Roman Comagmatic Region*; Carnegie Institution for Science: Washington, DC, USA, 1906; Volume 57, p. 199.
7. Stoppa, F.; Principe, C.; Schiazza, M.; Liu, Y.; Giosa, P.; Crocetti, S. Magma evolution inside the 1631 Vesuvius magma chamber and eruption triggering. *Open Geosci.* **2017**, *9*, 24–52. [CrossRef]
8. Lavecchia, G.; Stoppa, F. The Tirrenian zone: A case of lithosphere extention control of intra-continental magmatism. *Heart Planet. Sci. Lett.* **1990**, *99*, 336–350. [CrossRef]
9. Antonelli, F.; Nappi, G.; Lazzarini, L. Sulla «pietra da mole» della regione di Orvieto. Caratterizzazione petrografica e studio archeometrico di macine storiche e protostoriche dall'Italia centrale. Atti del I Congresso Nazionale di Archeometria (AIAr). *Pàtron Ed.* **2000**, *195*, 207.
10. Antonelli, F.; Nappi, G.; Lazzarini, L. Roman millstones from Orvieto (Italy): Petrographic and geochemical data for a new archaeometric contribution. *Archaeometry* **2001**, *43*, 167–189. [CrossRef]
11. Columbu, F.; Antonelli, F.; Sitzia, F. Origin of the Roma worked stones from St. Saturno Christian basilica, (Suoth Sardinia Italy). *Mediterr. Archaeol. Archaeom.* **2018**, *18*, 17–36.
12. Columbu, S.; Piras, G.; Sitzia, F.; Pagnotta, S.; Ranieri, S.; Legaioli, S.; Palleschi, V.; Lezzerini, M.; Giamello, M. Petrographyc and mineralogocal characterisation of volcanic rocks and surface-deposition of Romanesque monuments. *Mediterr. Archaeol. Archaeom.* **2018**, *18*, 37–64.
13. Appleton, J.D. Petrogenesis of potassiumrich lavas from the Roccamonfina Volcano, Roman Region, Italy. *J. Petrol.* **1972**, *13*, 425–456. [CrossRef]
14. Rogers, N.W.; Hawkesworth, C.J.; Parker, R.J.; Marsh, J.S. The geochemistry and petrogenensis of potassic lavas from Vulsini, Central Italy, and implication for mantle enrichment processes beneath the Roman region. *Contrib. Miner. Pet.* **1985**, *90*, 244–257. [CrossRef]

15. Giannetti, B.; Masi, U. Trace-element behavior during weathering of leucite in potassic rocks from the Roccamonfina volcano (Campania, southern Italy) and environmental implications. *Lithos* **1989**, *22*, 317–324. [CrossRef]
16. Giannetti, B.I. The extracaldera «Galluccio Tuff», Roccamonfina volcano, Italy. *Rend. Fis. Acc. Lincei* **1994**, *5*, 125–133. [CrossRef]
17. Giannetti, B. Comments on Cole et al. (1992). II The intracaldera «Galluccio Tuff» and «Garofali Formation». *Rend. Fis. Acc. Lincei* **1994**, *5*, 211–221. [CrossRef]
18. Di Battistini, G.; Montanini, A.; Vernia, L.; Bargossi, G.M.; Castorina, F. Petrology and geochemistry of ultrapotassic rocks from the Montefiascone Volcanic Complex (Central Italy): Magmatic evolution and petrogenesis. *Lithos* **1998**, *43*, 169–195. [CrossRef]
19. Perini, G.; Francalanci, L.; Davidson, J.P.; Conticelli, S. Evolution and genesis of magmas from Vico volcano, Central Italy: Multiple differentiation pathways and variable parental magmas. *J. Petrol.* **2004**, *45*, 139–182. [CrossRef]
20. Cundari, A. Petrogenesis of leucite-bearing lavas in the Roman volcanic Region, Italy. The Sabatini lavas. *Contrib. Mineral. Petrol.* **1979**, *70*, 9–21. [CrossRef]
21. Armienti, P.; Tonarini, S.; D'Orazio, M.; Innocenti, F. Genesis and evolution of Mount Etna alkaline lavas: Petrological and Sr-Nd-B isotope constraints. *Period. Mineral.* **2004**, *73*, 29–52.
22. Armienti, P.; Tonarini, S.; Innocenti, F.; D'Orazio, M. Mount Etna pyroxene as tracer of petrogenetic processes and dynamics of the feeding system. *Geol. Soc. Am. Spec.* **2007**, *418*, 265.
23. Isakovaa, A.T.; Panina, L.; Stoppa, F. Formation Conditions of Leucite-Bearing Lavas in the Bolsena Complex (Vulsini, Italy): Research data on melt inclusions in minerals. *Russ. Geol. Geophys.* **2019**, *60*, 119–132. [CrossRef]
24. Williamson, D.F.; Robert, A.; Parker, D.S.; Juliette, S. The Box Plot: A Simple Visual Method to Interpret Data. *Acad. Clin.* **1989**, *110*, 916–921. [CrossRef]
25. Liritzis, I.; Xanthopoulou, V.; Palamara, E.; Papageorgiou, I.; Iliopoulos, I.; Zacharias, N.; Vafiadou, A.; Karydas, A.G. Characterization and provenance of ceramic artifacts and local clays from late Mycenaean Kastrouli (Greece) by means of P-XRF screening and statistical analysis. *J. Cult. Herit.* **2020**, *46*, 61–81. [CrossRef]
26. Jolliffe, I.T. Principal Component Analysis. *Encycl. Stat. Behav. Sci.* **2005**, *3*, 1580–1584.
27. Ambrosio, F.A. A new statistical approach to the geochemical systematics of Italian alkaline igneous rocks. *Open Geosci.* **2020**, *12*, 133–147. [CrossRef]
28. Josse, J. Principal component methods- Hierarchical clustering, partitional clustering: Why would we need to choose for visalising data? *Mathematics* **2010**, *2010*, 1–17.
29. Le Bas, M.J.; Le Maitre, R.W.; Strekeisen, A.; Zanettin, B. A chemical classifcation of volcanic rocks based on the total alkali±silica diagram. *J. Petrol.* **1986**, *27*, 745–750. [CrossRef]
30. De La Roche, H.; Leterrier, J.T.; Grandclaude, P.; Marchal, M. A classification of volcanic and plutonic rocks using R1R2-diagram and major-element analyses its relationships with current nomenclature. *Chem. Geol.* **1980**, *29*, 183–210. [CrossRef]
31. Streckeisen, A. Classifcation and nomenclature of volcanics rocks, lamprophyres, carbonatites and melilitic rocks: Recommendations and suggestions of the IUGS. Subcommission on the systematics of igneous rocks, Geology. *Geol. Soc. Am. Boulder* **1979**. [CrossRef]
32. McDonough, W.F.; Sun, S.S. The composition of the Earth. *Chem. Geol.* **1995**, *120*, 223–253. [CrossRef]
33. Nakamura, N. Determination of REE, Ba, Fe, Mg, Na and K in carbonaceous and ordinary chondrites. *Geochim. Cosmochim. Acta* **1974**, *38*, 757–775. [CrossRef]
34. Castorina, F.; Stoppa, F.; Cundari, A.; Barbieri, M. An enriched mantle source for Italy's melilitite-carbonatite association as inferred by its Nd-Sr isotope signature. *Mineral. Mag.* **2000**, *64*, 625–639. [CrossRef]
35. Bell, K.; Lavcchia, G.; Rosatelli, G. Cenozoic Italian magamatism-Isotope constraints for possible plume-realte activity. *J. S. Am. Heart Sci.* **2013**, *41*, 22–40. [CrossRef]
36. Morelli, C. Gli avanzi Romani di Pagliano presso Orvieto. In *Bollettino dell'Istituto Storico Artistico Orvietano, anno XIII*; Tipografia Degli Orfanelli: Orvieto, Italy, 1957.
37. Bruschetti, P. Il porto di Pagliano tra Tevere e Paglia. In *The Tiber Valley in Antiquity*; Abstract Volume Book: Mercator Placidissimus the Tiber Valley in Antiquity, New Research in the Upper and Middle River Valley; Quasar: Rome, Italy, 2004; pp. 27–28.
38. Nappi, G.; Antonelli, F.; Coltorti, M.; Milani, L.; Renzulli, A.; Siena, F. Volcanological and petrological evolution of the Eastern Vulsini District, Central Italy. *J. Volcanol. Geotherm. Res.* **1998**, *87*, 211–232. [CrossRef]
39. Renzulli, A.; Antonelli, F.; Santi, P.; Busdraghi, P.; Luni, M. Provenance determination of lava paving stones from the Roman 'Via Consolare Flaminia' pavement (Central Italy) using petrological investigations. *Archaeometry* **1999**, *41*, 209–260. [CrossRef]
40. Renzulli, A.; Santi, P.; Nappi, G.; Luni, M.; Vitali, D. Provenance and trade of volcanic rock millstones from Etruscan-Celtic and Roman archaeological sites in Central Italy. *Eur. J. Mineral.* **2002**, *14*, 175–183. [CrossRef]
41. Cristofolini, R.; Romano, R. Petrologic features of the Etnean volcanic rocks. *Mem. Soc. Geol. Ital.* **1982**, *23*, 99–115.
42. McCallum, M. The supply of stone of the site of Rome: A case study of the transport of anician building stone and millstone from the Santas trinità quarry (Orvieto). In *Trade and Exchange: Archaeologiocal Studies from History and Prehistory*; White, C., Dillian, C., Eds.; Springer: Berlin/Heidelberg, Germany, 2010; pp. 75–94.
43. Oliva, P.; BeÂziat, D.; Domergue, C.; Jarrier, C.; Martin, F.; Pieraggi, B.; Tollon, F. Geological sources and use of rotary millstones from the Roman iron-making site of Les Martys (Montagne Noire, France). *Eur. J. Mineral.* **1999**, *11*, 757–762. [CrossRef]
44. Corsaro, R.; Cristofolini, R.; Pezzino, A.; Sergi, A. Evidence for the provenance of building stone of igneous origin in the Roman Theatre in Catania. *Per. Mineral.* **2000**, *69*, 239–255.

45. Cristofolini, R.; Corsaro, R.A.; Ferlito, C. Variazioni petrochimiche nella successione etnea: Un riesame in base a nuovi dati da campioni di superficie e da sondaggi. *Acta Vulcanol.* **1991**, *1*, 25–37.
46. Williams, O.; Thorpe, R. Millstones that mapped the Mediterranean. *New Sci.* **1991**, *129*, 34–37.
47. Galadini, F.; Falcucci, E.; Campanelli, A. Tracce archeologiche di un terremoto tardo antico nella Piana del Fucino (Italia centrale). In Proceedings of the Gruppo Nazionale di Geofisica della Terra Solida, 27° Congress Trieste, Trieste, Italy, 6 October 2008.
48. Stoppa, F. Ten Years of Geo-Archeo-Mythological Studies in the Abruzzo Region—Central Italy: An Updated Review. *Open Access J. Archaeol. Anthropol.* **2020**. [CrossRef]